A Simple Hybrid Model for Estimating Remaining Useful Life of SiC MOSFETs in Power Cycling Experiments

Mattias P. Eng[1*], Andreas Lövberg[2], Maciej Misiorny[3], Madhav Mishra[4], Wilhelm Söderkvist Vermelin[5], and Klas Brinkfeldt[6]

[1,2,4,5,6] *RISE – Research Institutes of Sweden, Mölndal, SE-431 53, Sweden*

mattias.eng@ri.se
andreas.lovberg@ri.se
madhav.mishra@ri.se
wilhelm.soderkvist.vermelin@ri.se
klas.brinkfeldt@ri.se

7103

[3] *QRTECH AB, Mölndal, SE-431 35, Sweden*

maciej.misiorny@qrtech.se

Abstract

Recording and prediction of the accumulated damage, which will eventually lead to the failure of power electronic modules, is an aspect of high importance for power electronic systems design and, in particular, for development of Prognostic and Health Management (PHM) schemes for in-field applications. To this end, this paper presents a simple and cost-effective prognostic method for predicting the remaining useful life (RUL) of TO-247 packaged silicon carbide (SiC) metal-oxide semiconductor field-effect transistors (MOSFETs) subjected to power cycling experiments. The model assumes that the major failure mode is bond-wire lift-off and uses a damage accumulation scheme based on Paris' crack law. The only inputs to the model are historical data on the average junction temperature swing and the temperature-compensated drain-source ON-state resistance at the peak temperature of the current cycle. Using only these two input values, the model is shown to predict RUL with surprising accuracy for the range of constant current loads determining cycling conditions under which the test data series have been acquired. This work is a first step in an ongoing project towards building more elaborate prognostic schemes for RUL-determination of SiC power MOSFETs in actual working conditions, using physics-informed neural networks (PINNs).

1. Background

Power electronic systems and components play an increasingly important role in upholding many basic functions that we take for granted in our everyday lives. They provide compact and efficient solutions to power conversion in applications such as utility interfaces with energy resources, energy storage systems, unified power quality correction, and electric or hybrid electric vehicles. Most power electronic systems, however, are not equipped with redundancy. In consequence, any fault that occurs to the components will inevitably result in a shutdown of the entire system. Such unscheduled interruptions not only cause significant safety concerns – particularly in health care, aerospace, and automotive applications – but also increase the operational costs – for example in off-shore wind farms and other power production applications.

In general, system failures are hardly ever completely preventable. For this reason, the preferred approach is to act before a failure occurs, and models for prediction of remaining useful life, if applied appropriately, can fulfill this task. To achieve this, the development of device-specific models for RUL estimation is required. Empirical or semi-empirical approaches, often based on Arrhenius type expressions, have traditionally been employed to estimate the expected lifetime of components. Such models have been shown to accurately forecast the average failure rates for a large sets of devices over broad ranges of physical conditions (Bayerer et al., 2008; Hanif et al., 2019). However, when applied to single devices, the predictive capabilities of such models are typically very limited and subject to large errors. In contrast, prognosticating models based on Machine Learning (ML) algorithms have been demonstrated to be able to estimate RUL for single devices with great accuracy (Söderkvist Vermelin et al., 2023). A big drawback associated with ML-based methods is that the

Mattias P. Eng et al. This is an open-access article distributed under the terms of the Creative Commons Attribution 3.0 United States License, which permits unrestricted use, distribution, and reproduction in any medium, provided the original author and source are credited.

variables and relationships resulting from the training don't allow for obtaining a straightforward interpretation. Furthermore, if an ML-based algorithm is faced with data collected under operational conditions that differ significantly from those of the dataset used for training the algorithm, the performance deteriorates (Hendrycks et al., 2021; Lakshminarayanan et al., 2017; Söderkvist Vermelin et al., 2023). A possible solution for overcoming this problem is to use physics informed ML models, where a model based on Physics-of-Failure (PoF) sets certain constraints for the algorithm. Such a combination has the potential for yielding accurate RUL predictions on a device level, while still maintaining the ability to extrapolate outside the training conditions.

The most vulnerable elements in power electronic systems are the power semiconductor devices and electrolytic capacitors (Song & Wang, 2013). These components are built up of layers of materials characterized by different coefficients of thermal expansion (CTE), which, in turn, leads to thermo-mechanical stress arising between adjacent layers due to temperature variations over time. This thermo-mechanical stress is the primary cause for the accumulation of damage. In the case of power MOSFETs the main failure mechanism is bond-wire lift-off which results from cracks in the interface between wire-bond and the metallization layer. Interestingly, Paris' law (Paris & Erdogan, 1963) – a simple analytical expression for estimating crack propagation during cyclic loading – has been shown to be a good candidate for combining physical models with particle filters to predict RUL for bond-wires in Si-based insulated gate bipolar transistors (IGBTs) (Hu et al., 2020; Lu & Christou, 2019). This result inspired us to adopt such an approach for the development of a PINN-based RUL prediction scheme for SiC MOSFETs, which is the topic of this work. As a first step towards this, we here present a simple RUL prediction scheme with three fitting parameters and apply this to a set of data from power cycling experiments.

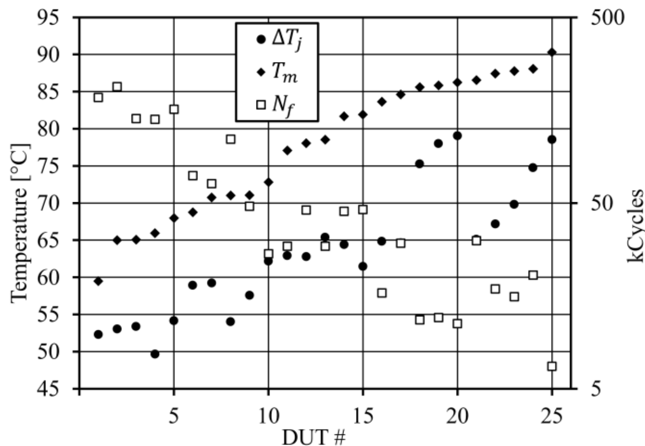

Figure 1. The resulting parameters; T_m, ΔT_j, and N_f acquired for the 25 DUTs in the study.

Table 1. Power cycling parameters for the different runs in this study.

Run	Number of DUTs	Set current [A]	Measured current [A]
1	10	23	22.9
2	10	24	23.7
3	5	26	25.7

2. EXPERIMENTAL

In this study, we induced wire-bond degradation in 25 silicon carbide (SiC) TO-247 packaged power MOSFETs using power cycling. The power cycling system used was from Hollander Research, and the SiC MOSFETs were being continuously thermally stabilized via a water-cooled mounting block. The power cycling was performed in three series, each corresponding to a different current load, as illustrated by Tab. 1. During the power cycling procedure, the drain-source ON-state voltage and a range of various temperatures were recorded.

Please refer to a joint paper submitted to ESREL2023 for more details (Söderkvist Vermelin et al., 2023). In the present work, the temperature measured at the drain leg will be used as an approximation of the junction temperature, T_j. This temperature was measured every 90 cycles leading to an estimation of the junction temperature swing, the difference between the temperature at the end of and at the beginning of the ON-state period in each cycle, ΔT_j. Values for ΔT_j between each measurement were then estimated by linear interpolation.

The different loading levels and positions on the mounting block, as well as variations in device quality, resulted in a range of mean drain leg temperatures (T_m) and ΔT_j for each device under test (DUT). The power cycling was carried out until all devices in each run failed, with the failure criterion being defined by a change in temperature-compensated drain-source ON-state resistance exceeding 5%. As a result, the total number of cycles till failure (N_f) together with run-to-failure trajectories were obtained for each DUT. The resulting key parameters are compiled in Fig. 1. The devices were numbered between 1 and 25 in order of increasing T_m.

The temperature-compensated difference in ON-state resistance ($\Delta R_{DS,on}$) was derived using the temperature measured on the mounting block (T_b) as follows: First, a device-specific dependence of the ON-state resistance ($R_{DS,on}$) on T_b was determined for each DUT based on data from the initial 200 cycles. This function essentially describes how $R_{DS,on}$ should vary with temperature for an undegraded ("healthy") device. Second, the actual $R_{DS,on}$ and corresponding T_b at the end of the current pulse were collected for all cycles. Note that this resistance contains

information about how degradation of a device progresses with its power cycling. Next, using the collected T_b and the device-specific dependence of resistance on temperature mentioned above, the hypothetical "healthy" $R_{DS,on}$ was calculated for all cycles. Finally, $\Delta R_{DS,on}$ was obtained as the difference between the measured $R_{DS,on}$ and the value expected from a "healthy" device.

Data handling and simulations were performed in Python (Van Rossum & Drake, 2009) where the optimizations of the various parameters described in the model below were performed using the using the `optimize.minimize` module implemented in the SciPy package (Virtanen et al., 2020).

3. THE MODEL

As described above, the model considered in this paper assumes that bond-wire lift-off is the dominant failure mechanism, which is caused by the propagation of a crack in the wire "footprint" right at the interface between the bond-wire and the metallization layer. For Si IGBTs, this mechanism has been shown to take place simultaneously from both sides in a symmetrical manner, as is illustrated in Fig. 2 (Dornic et al., 2018, 2020).

The process of crack growth under cyclic loading can in general be divided into three phases: crack initiation, crack propagation, and structural fracture, as schematically illustrated in Fig. 3 (Benguediab et al., 2012). The first stage presents a threshold below which there is no crack growth. In the second stage, the crack growth rate increases exponentially with respect to the number of cycles (see the linear region in Fig. 3) and in the final stage the system reaches the unstable state in which the structure fails within a small number of cycles.

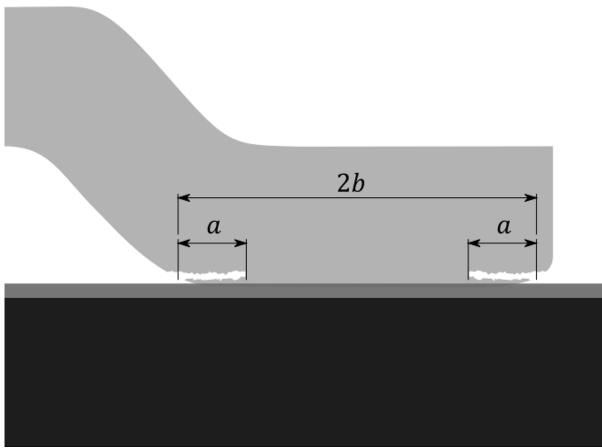

Figure 2. An illustration of a crack, of length a, propagating above the interface between the wire and the metallization layer in a wire-bond with a footprint of length $2b$.

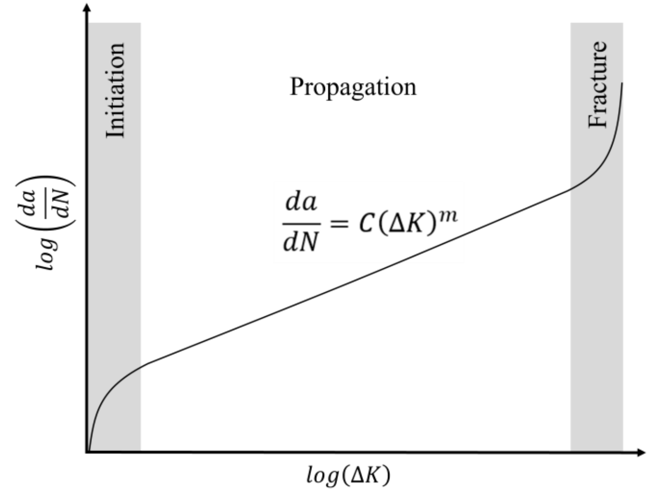

Figure 3. The three stages of crack growth; initiation, propagation, and fracture.

When modelling crack propagation in wire-bonds, the first stage is commonly assumed to be of minor importance, whereas failure during the last stage is so rapid that the RUL is in practice close to zero once this is reached. Consequently, the lifetime of the bond-wire can be regarded as the lifetime of the propagating crack, which is described by Paris' law:

$$\frac{da}{dN} = C(\Delta K)^m \tag{1}$$

Here, a is the crack length, N represents the cycle number, ΔK stands for the effective stress intensity range, while C and m are material constants. In general, ΔK depends on factors such as: localized geometry, current crack length, material and environmental parameters, as well as cyclic stress, and it can be approximated as follows: (Tada et al., 2000).

$$\Delta K = \Delta\sigma\sqrt{\pi a} \cdot f(a/b) \tag{2}$$

where $\Delta\sigma$ represents the effective stress range and $f(a/b)$ is a function depending on a and, in the present case half, the width of the sample (b). Note that $\Delta\sigma$ is primarily governed by the CTE mismatch between SiC and the bond-wire, and thus by ΔT_j. In consequence, for a given device, ΔK is therefore determined by of ΔT_j and a:

$$\Delta K = g(\Delta T_j) \cdot \sqrt{\pi a} \cdot f(a/b) \tag{3}$$

The function, $f(a/b)$, has been determined experimentally for various crack propagation scenarios (Tada et al., 2000). In the case of double edge notch test specimens, which is most like the conditions illustrated in Fig. 2, the function under discussion can with good accuracy be approximated as:

$$f(a/b) = \\ = \frac{e_1 - e_2 \frac{a}{b} - e_3 \left(\frac{a}{b}\right)^2 + e_4 \left(\frac{a}{b}\right)^3 - e_5 \left(\frac{a}{b}\right)^4}{\sqrt{1 - \frac{a}{b}}} \quad (4)$$

where the phenomenological constants, from e_1 to e_5, are 1.122, 0.56, 0.205, 0.471, and 0.19, respectively, and b is half of the total width of the specimen, which in the present scenario corresponds to the bond-wire "footprint" (see Fig. 2). On the other hand, for the function g a simple power dependence on ΔT_j was tested and proved to be compatible with physically reasonable values for C and m:

$$g(\Delta T_j) = c\Delta T_j^d \quad (5)$$

where c and d are fitting parameters. Using the equations introduced above, Paris' law can be reformulated into a discrete form representing a cumulative damage model that describes the crack length after N cycles (where $c\sqrt{\pi}$ have been incorporated into C):

$$a_N = a_{N-1} + C\left(\Delta T_j^d \cdot \sqrt{a_{N-1}} \cdot f(a_{N-1}/b)\right)^m \quad (6)$$

Optimization of the parameters C, m, and d, to give the best fit of Eq. 6 to the experimental data was performed in the following manner: a_N was calculated, starting with values for the parameters inspired by literature (Hanif et al., 2019; Paris & Erdogan, 1963) and using a value of the initial crack length (a_0) of 0.02 mm. This procedure was repeated for each DUT until either $a_{N+1} \geq b$ or $N + 1 > N_f$. The sum of the errors, $N - N_f$ and $a_N - b$, for all DUTs were then minimized which resulted in the fit shown in Fig. 4.

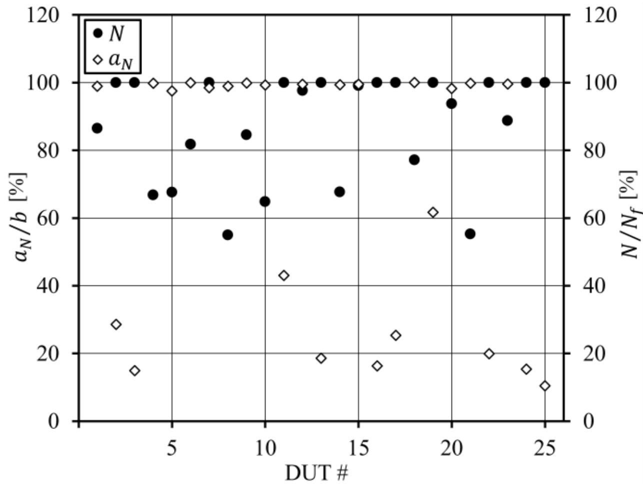

Figure 4. A visualization of the resulting errors after optimizing the parameters C, d, and m, in Eq. 6 to match the experimental values N_f and b.

The values of parameters C, d, and m, obtained by means of the optimization procedure, are $8.48 \cdot 10^{-17}$, 2.12, and 3.27, respectively. Importantly, the value derived for m falls in the range between 3 and 4 commonly observed for aluminium alloys (Benguediab et al., 2012; Paris & Erdogan, 1963; Sasaki et al., 2008).

Since there is no direct way to measure the crack length when a DUT is in operation, the next step is to identify a suitable parameter that can give an experimental estimate of the accumulated damage. The temperature-compensated ON-state voltage, at constant current load, has previously been identified as a suitable candidate (Degrenne & Mollov, 2018; Hanif et al., 2019; Hu et al., 2020). Because the data set used in this work is the result of power cycling at different currents, the temperature-compensated drain-source ON-state resistance, $R_{DS,on}$, measured at the end of each cycle will be instead employed as a damage indicator. The dependence of $R_{DS,on}$ on a_N is given by (Degrenne & Mollov, 2018):

$$\left(R_{DS,on}\right)_N = r_0 + \frac{r_1}{1 - r_a \cdot a_N} \quad (7)$$

where r_0, r_1, and r_a are DUT-specific parameters. Thus, the change in $R_{DS,on}$ at cycle N relative to an undamaged DUT can be described by:

$$\left(\Delta R_{DS,on}\right)_N = \frac{r_1}{1 - r_a \cdot a_N} - r_1 \quad (8)$$

Finally, by combining Eqs. 6 and 8, estimates of the parameters r_a and r_1 for each DUT, can be derived in the following manner. Firstly, DUT-specific crack propagation trajectories were generated. This was achieved by using the same optimization procedure as described above except that the parameters C, m, and d, were kept constant while fitting a DUT-specific a_0. This procedure resulted in DUT-specific values of a_0 in the range of 0.02 ± 0.01. Secondly, the crack propagation trajectories, given by Eq. 6, were incorporated into Eq. 8, yielding the corresponding ON-state resistance change trajectories, $\left(\Delta R_{DS,on,fit}\right)_N$.

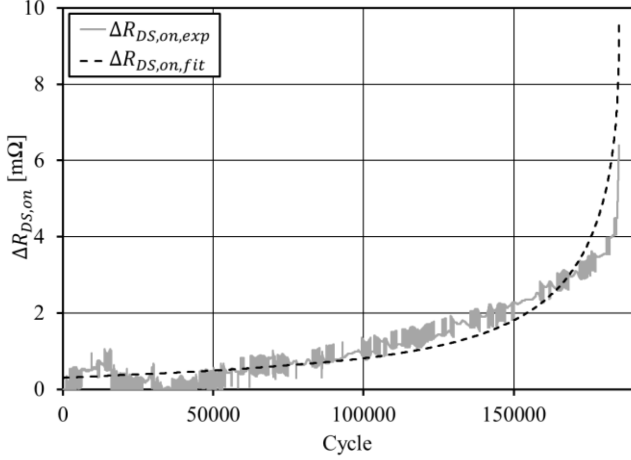

Figure 5. The measured $\Delta R_{DS,on}$ as a function of cycle number and a fit of the device specific parameters a_0, r_a, and r_1 using Eqs. 6 and 8 for DUT #1.

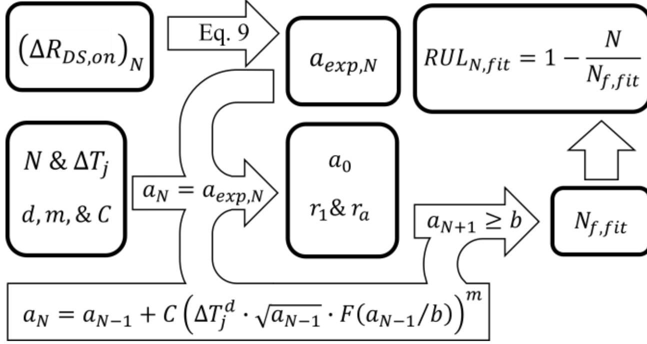

Figure 6. RUL estimation at cycle N, using the measured $\Delta R_{DS,on}$ and ΔT_j and the pre-determined parameters (d, m, and C) by fitting device specific parameters (r_a, a_0, and r_1).

The DUT-specific parameters r_a and r_1 were derived by minimizing the mean square error between the measured (experimental) and modelled trajectories. As a result, a set of individual fits were obtained, and an example fit for DUT #1 is shown in Fig. 5. The derived DUT-specific r_a and r_1 values are in the range of 0.02 ± 0.005 and 1.6 ± 0.2, respectively.

A complete toolset for estimating RUL on the go, using the measured ΔT_j and $(\Delta R_{DS,on})_N$, has now been derived. The proposed procedure is schematically illustrated in Fig. 6 and can be summarized as follows: Firstly, at any given cycle, the measured $(\Delta R_{DS,on})_N$ gives an experimental value for the crack length via a rearrangement of Eq. 8:

$$a_{exp,N} = \frac{1}{r_a}\left(1 - \frac{r_1}{\left((\Delta R_{DS,on})_N + r_1\right)}\right) \tag{9}$$

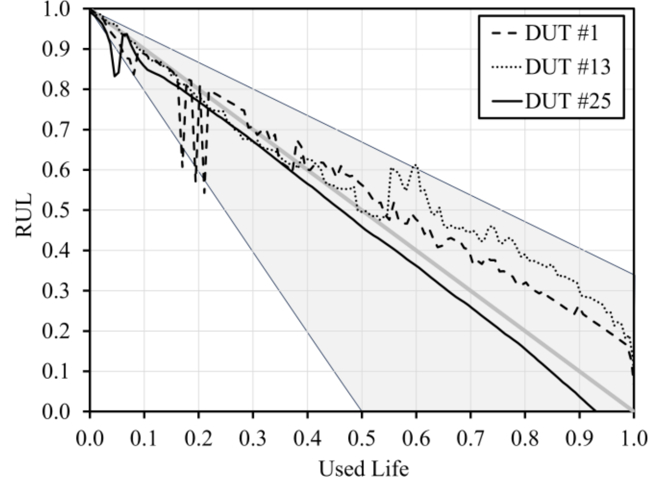

Figure 7. RUL determination using the model for DUTs #1, #13, and #25 with 185 294, 29 255, and 6 614 cycles till failure, respectively. The shaded area represents the uncertainty of prediction using the LESiT model.

Secondly, N and the series of ΔT_j lead to a prediction of a_N via Eq. 6, using the pre-determined parameters C, d, and m. Starting with the mean values for r_a, a_0, and r_1 and then minimizing the error $a_N - a_{exp,N}$ by varying the parameters within the previously determined ranges as bounds, result in new N-specific values for the parameters. Using the N-specific a_0 in Eq. 6 and iterating until the criterion $a_{N+1} \geq b$ is met yields a prediction of the total number of cycles till failure, $N_{f,fit}$. Finally, the RUL can be straightforwardly derived with the use of $N_{f,fit}$ (see Fig. 6).

4. RESULTS

To illustrate the RUL prediction capabilities of the simple model described above, three DUTs, that is, #1, #13, and #25, with lowest, middle, and highest T_m, respectively, were analyzed. Since the total number of cycles till failure differ significantly for the chosen devices: 185 294, 29 255, and 6 614, the RUL was estimated every 1000, 200, and 50 cycles for the three DUTs, respectively. The resulting estimated RULs plotted as a function of consumed life is shown in Fig. 7. As a comparison the data was also fitted to the LESiT model (Held et al., 1997), an Arrhenius-type model representing traditional lifetime predictions. The fit resulted in a ± 50% uncertainty in the prediction of N_f, leading to a span of RUL predictions illustrated by the shaded area in Fig. 7.

5. CONCLUSION

We have demonstrated that a simple model based on damage accumulation using Paris' law for crack propagation is capable of predicting RUL for SiC power MOSFETs in constant load power cycling experiments to a good degree using only the junction temperature swing and temperature-

compensated ON-state resistance. The model has been minimized in terms of data storage and parameters and is very computationally cheap. This is because it only involves the optimization of three parameters within quite narrow intervals. Consequently, it only requires the temperature-compensated ON-state resistance of a “healthy” DUT, and the same for the power cycle of interest, along with the junction temperature swings to estimate the RUL of the current cycle. The use of the model outside the very regular periodic conditions of power cycling experiments, however, is expected to be very limited. To improve the model for more challenging conditions it will have to be refined with more flexibility. This can be done either by including cycle-to-cycle interactions or by implementing it in PINNs where the parameter optimization procedure could be replaced with a neural network that can model complex functions. This would make the method more general and parameter estimations could be made from complex, multivariate sensor measurements where the underlying physical laws might not be known.

ACKNOWLEDGEMENT

This research is conducted within the iRel4.0 Intelligent Reliability project, which is funded by Horizon 2020 Electronics Components for European Leadership Joint Undertaking Innovation Action (H2020-ECSELJU-IA). This work is also funded by the Swedish innovation agency Vinnova, through co-funding of H2020-ECSEL-JU-IA.

REFERENCES

Bayerer, R., Herrmann, T., Licht, T., Lutz, J., & Feller, M. (2008). Model for Power Cycling lifetime of IGBT Modules—Various factors influencing lifetime. *5th International Conference on Integrated Power Electronics Systems*, 1–6.

Benguediab, M., Bouchouicha, B., Mokhtar, Z., & Mazari, M. (2012). Crack propagation under constant amplitude loading based on an energetic parameters and fractographic analysis. *Materials Research*, *15*, 544–548. https://doi.org/10.1590/S1516-14392012005000072

Degrenne, N., & Mollov, S. (2018). Diagnostics and Prognostics of Wire-Bonded Power Semi-Conductor Modules subject to DC Power Cycling with Physically-Inspired Models and Particle Filter. *PHM Society European Conference*, *4*(1), Article 1. https://doi.org/10.36001/phme.2018.v4i1.167

Dornic, N., Ibrahim, A., Khatir, Z., Degrenne, N., Mollov, S., & Ingrosso, D. (2020). Analysis of the aging mechanism occurring at the bond-wire contact of IGBT power devices during power cycling. *Microelectronics Reliability*, *114*, 113873. https://doi.org/10.1016/j.microrel.2020.113873

Dornic, N., Ibrahim, A., Khatir, Z., Tran, S. H., Ousten, J.-P., Ewanchuk, J., & Mollov, S. (2018). Analysis of the degradation mechanisms occurring in the topside interconnections of IGBT power devices during power cycling. *Microelectronics Reliability*, *88–90*, 462–469. https://doi.org/10.1016/j.microrel.2018.07.041

Hanif, A., Yu, Y., DeVoto, D., & Khan, F. (2019). A Comprehensive Review Toward the State-of-the-Art in Failure and Lifetime Predictions of Power Electronic Devices. *IEEE Transactions on Power Electronics*, *34*(5), 4729–4746. https://doi.org/10.1109/TPEL.2018.2860587

Held, M., Jacob, P., Nicoletti, G., Scacco, P., & Poech, M.-H. (1997). Fast power cycling test of IGBT modules in traction application. *Proceedings of Second International Conference on Power Electronics and Drive Systems*, *1*, 425–430 vol.1. https://doi.org/10.1109/PEDS.1997.618742

Hendrycks, D., Basart, S., Mu, N., Kadavath, S., Wang, F., Dorundo, E., Desai, R., Zhu, T., Parajuli, S., Guo, M., Song, D., Steinhardt, J., & Gilmer, J. (2021). The Many Faces of Robustness: A Critical Analysis of Out-of-Distribution Generalization. *2021 IEEE/CVF International Conference on Computer Vision (ICCV)*, 8320–8329. https://doi.org/10.1109/ICCV48922.2021.00823

Hu, K., Liu, Z., Du, H., Ceccarelli, L., Iannuzzo, F., Blaabjerg, F., & Tasiu, I. A. (2020). Cost-Effective Prognostics of IGBT Bond Wires With Consideration of Temperature Swing. *IEEE Transactions on Power Electronics*, *35*(7), 6773–6784. https://doi.org/10.1109/TPEL.2019.2959953

Lakshminarayanan, B., Pritzel, A., & Blundell, C. (2017). *Simple and Scalable Predictive Uncertainty Estimation using Deep Ensembles* (arXiv:1612.01474). arXiv. https://doi.org/10.48550/arXiv.1612.01474

Lu, Y., & Christou, A. (2019). Prognostics of IGBT modules based on the approach of particle filtering. *Microelectronics Reliability*, *92*, 96–105. https://doi.org/10.1016/j.microrel.2018.11.012

Paris, P., & Erdogan, F. (1963). A Critical Analysis of Crack Propagation Laws. *Journal of Basic Engineering*, *85*(4), 528–533. https://doi.org/10.1115/1.3656900

Sasaki, K., Iwasa, N., Kurosu, T., Saito, K., Koike, Y., Kamita, Y., & Toyoda, Y. (2008). Thermal and Structural Simulation Techniques for Estimating Fatigue Life of an IGBT Module. *2008 20th International Symposium on Power Semiconductor Devices and IC's*, 181–184. https://doi.org/10.1109/ISPSD.2008.4538928

Söderkvist Vermelin, W., Lövberg, A., Misiorny, M., Eng, M. P., & Brinkfeldt, K. (2023). Data-Driven Remaining Useful Life Estimation of Discrete

Power Electronic Devices. *European Safety and Reliability Conference*, In press.

Song, Y., & Wang, B. (2013). Survey on Reliability of Power Electronic Systems. *IEEE Transactions on Power Electronics*, *28*(1), 591–604. https://doi.org/10.1109/TPEL.2012.2192503

Tada, H., Paris, P. C., & Irwin, G. R. (2000). *The Stress Analysis of Cracks Handbook, Third Edition*. https://doi.org/10.1115/1.801535

Van Rossum, G., & Drake, F. L. (2009). *Python 3 Reference Manual*. CreateSpace.

Virtanen, P., Gommers, R., Oliphant, T. E., Haberland, M., Reddy, T., Cournapeau, D., Burovski, E., Peterson, P., Weckesser, W., Bright, J., van der Walt, S. J., Brett, M., Wilson, J., Millman, K. J., Mayorov, N., Nelson, A. R. J., Jones, E., Kern, R., Larson, E., … van Mulbregt, P. (2020). SciPy 1.0: Fundamental algorithms for scientific computing in Python. *Nature Methods*, *17*(3), Article 3. https://doi.org/10.1038/s41592-019-0686-2